Available online at www.sciencedirect.com
SCIENCE DIRECT®
Advances in Space Research 35 (2005) 711–724
ADVANCES IN SPACE RESEARCH (a COSPAR publication)
www.elsevier.com/locate/asr

Large scale MHD properties of interplanetary magnetic clouds

S. Dasso [a,*,1], C.H. Mandrini [a], P. Démoulin [b], M.L. Luoni [a], A.M. Gulisano [a]

[a] Instituto de Astronomía y Física del Espacio (IAFE), CONICET-UBA, Ciudad Universitaria, CC. 67 Suc. 28, 1428 Buenos Aires, Argentina
[b] Observatoire de Paris, LESIA, UMR 8109 (CNRS), F-92195 Meudon Cedex, France

Received 31 May 2004; received in revised form 10 February 2005; accepted 22 February 2005

Abstract

Magnetic Clouds (MCs) are the interplanetary manifestation of Coronal Mass Ejections. These huge astrophysical objects travel from the Sun toward the external heliosphere and can reach the Earth environment. Depending on their magnetic field orientation, they can trigger intense geomagnetic storms. The details of the magnetic configuration of clouds and the typical values of their magnetohydrodynamic magnitudes are not yet well known. One of the most important magnetohydrodynamic quantities in MCs is the magnetic helicity. The helicity quantifies several aspects of a given magnetic structure, such as the twist, kink, number of knots between magnetic field lines, linking between magnetic flux tubes, etc. The helicity is approximately conserved in the solar atmosphere and the heliosphere, and it is very useful to link solar phenomena with their interplanetary counterpart. Since a magnetic cloud carries an important amount of helicity when it is ejected from the solar corona, estimations of the helicity content in clouds can help us to understand its evolution and its coronal origin. In situ observations of magnetic clouds at one astronomical unit are in agreement with a local helical magnetic structure. However, since spacecrafts only register data along a unique direction, several aspects of the global configuration of clouds cannot be observed. In this paper, we review the general properties of magnetic clouds and different models for their magnetic structure at one astronomical unit. We describe the corresponding techniques to analyze in situ measurements. We also quantify their magnetic helicity and compare it with the release of helicity in their solar source for some of the analyzed cases.

Keywords: Magnetic clouds; Coronal mass ejections; Magnetohydrodynamics; Magnetic helicity

1. Introduction

1.1. CMEs and ICMEs

Coronal Mass Ejections (CMEs) are massive expulsions of magnetized plasma from the solar atmosphere, due to a destabilization of the coronal magnetic configuration. As a consequence of this ejection, CMEs can form confined magnetic structures with both extremes of the magnetic field lines connected to the solar surface, extending far away from the Sun into the solar wind, while the coronal magnetic field is restructured in the low-corona. Depending on the solar cycle phase, about 3.5 (0.2) CMEs are ejected per day during a solar maximum (minimum), and the ejected mass can reach values as high as $\sim 10^{15}$–10^{16} g (e.g., Gosling, 1990, 1997).

Solar Ejecta (also known as Interplanetary Coronal Mass Ejections, ICMEs) are the interplanetary manifestation of CME events. They are transient structures that perturb the solar wind, as they move away from the Sun. When ejected in the Earth direction, depending on their orientation, ICMEs can initiate intense geomagnetic

* Corresponding author. Tel.: +54 11 4787 2712; fax: +54 11 4576 3371.
E-mail address: dasso@df.uba.ar (S. Dasso).
[1] Departamento de Física, FCEN, UBA, 1428 Buenos Aires, Argentina.

0273-1177/$30 © 2005 COSPAR. Published by Elsevier Ltd. All rights reserved.
doi:10.1016/j.asr.2005.02.096

perturbations as a consequence of reconnection processes in the terrestrial magnetopause (see e.g., Farrugia et al., 1997; Gonzalez et al., 1999 and references therein).

After several decades of in situ measurements, magnetic field and plasma properties, which are significantly different from that of the typical solar wind, have been determined for ICMEs.

The proton temperature (T_p) in ICMEs is abnormally lower than in the solar wind (see, e.g., Gosling, 1990; Richardson and Cane, 1995 and references therein).

The presence of parallel and/or antiparallel (to the magnetic field lines) flows of suprathermal protons with energies from a few keVs to ~1 MeV (Gosling et al., 1981; Marsden et al., 1987; Galvin et al., 1987) and parallel and/or antiparallel flows of suprathermal (energy $E \sim 80$–1000 eV) electrons (Montgomery et al., 1974; Bame et al., 1981; Gosling et al., 1987) can be observed when a spacecraft crosses an ICME. The presence of these streams (along the field lines) is generally viewed as a signature of field lines connected to the Sun (Gosling et al., 1987; Larson et al., 1997).

The α-particle to proton density ratio is highly variable in ICMEs, and may be very different from the typical 4% observed in the solar wind, reaching values as high as ~20% (Borrini et al., 1982; Galvin et al., 1987). Occasionally, enhancements of other minority ions are also observed in ICMEs (Galvin et al., 1987). Such enrichment suggests that the plasma inside the ICMEs originates in the low corona.

The proton population in the majority of ICMEs is such that $T_{\parallel} > T_{\perp}$, where $\parallel$ and $\perp$ denote directions parallel and perpendicular to the magnetic field (Zwickl et al., 1983; Gosling et al., 1987; Galvin et al., 1987). Electrons show a similar trend but with lower anisotropies (Pilipp et al., 1987; Gosling et al., 1987). This trend in the thermal anisotropy is consistent with the motion of charged particles in an expanding magnetic cloud (MC), as follows. Due to conservation of energy and magnetic moment of charged particles traveling toward a region with a weaker magnetic field that changes slowly, comparing with their cyclotron period, particles will tend to increase the parallel velocity taking energy from the perpendicular one (see, e.g., Baumjohann and Treumann, 1996).

Cane and Richardson (2003) have analyzed a large set of ICMEs in the near-Earth solar wind during 1996–2002, identifying them only from their interplanetary properties observed in situ. They found that the ICME rate increases by about one order of magnitude from solar minimum (~5 ICME per year) to solar maximum (~50 per year).

1.2. Magnetic clouds

The important subset of ICMEs known as interplanetary magnetic clouds (MCs), a term introduced by Burlaga et al. (1981), is characterized by enhanced magnetic field strengths with respect to ambient values, a smooth and large rotation of the magnetic field vector, and low T_p (e.g., Burlaga et al., 1981; Klein and Burlaga, 1982; Burlaga, 1990, 1995). The relative importance between the proton pressure against the magnetic pressure is measured by the proton plasma β_p parameter, being β_p the proton to the magnetic pressure ratio, $\beta_p = 8\pi k_B n_p T_p / B^2$, where $B = |\vec{\mathbf{B}}|$ is the magnetic field intensity, k_B is the Boltzman's constant, and n_p is the proton density. Since, by definition, MCs are objects with high magnetic field and low proton temperature, the mean value of β_p in MCs is frequently low, typically $\beta_p \sim 0.1$ (Lepping et al., 2003). However, values of $\beta_p \sim 0.2$–0.4 or even higher (see, e.g., Dasso et al., 2001) have been observed in clouds.

Fig. 1 shows a scheme of a magnetic cloud when it passes near the Earth. Inside the MC, the magnetic field lines form a helical structure (the so-called magnetic flux rope). The 'feet' of the flux rope can be attached or detached from the Sun, as shown by the dashed lines in the figure. This magnetic configuration is very different from the typical solar wind, whose magnetic configuration is basically the Parker's spiral (see, e.g., Hundhausen, 1995).

The electron temperature, T_e, is frequently higher than the proton temperature in MCs (Gosling et al., 1987; Galvin et al., 1987; Pilipp et al., 1987; Osherovich et al., 1993; Richardson et al., 1997). In particular, in the statistical study by Richardson et al. (1997) it has been suggested that $T_e/T_p > 2$ is a criterion to identify ICMEs. In some cases, T_e/T_p reaches values as high as 7–10 (Osherovich et al., 1993). So, the electron pressure can play a significant role in the magnetic configuration of MCs.

The level of magnetic fluctuations in MCs is generally lower than in the typical solar wind.

Magnetic Clouds

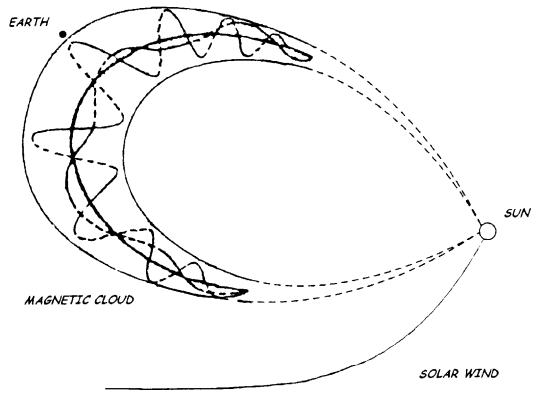

Fig. 1. Schematic global view of a magnetic cloud. The dashed lines indicate that the field lines can be attached or detached from its solar source when the cloud is observed in situ at 1 AU.

The mean free path along the magnetic field lines of some MCs can reach values as large as ~10 AU for energetic protons of ~20 MeV (Torsti et al., 2004), indicating that the flux rope structure of an ICME can provide a kind of 'highway' to some solar energetic particles. However, a non-negligible degree of fluctuations has been reported (Janoo et al., 1998). Moreover, since inside some MCs the thermal anisotropy is negative and the electrons are hotter than the protons, there are theoretical reasons (this physical scenario favors the slow down of the phase speed of the wave and so more ions can resonate) to expect the emission/absorption of electromagnetic waves in the ion-cyclotron frequency due to wave-particle resonances (Dasso et al., 2003a).

There is not yet an agreement on the criterion to identify the boundaries of MCs. Farrugia et al. (2001) identified a rotational discontinuity and a slow shock before the magnetic hole in front of one MC and interpreted the whole structure as a reconnection layer according to the Petshek-type reconnection theory. Planar magnetic structures have been observed in the upstream sheath, and have been interpreted as the result of the compression and draping of the heliospheric magnetic field when a fast MC propagates into the interplanetary medium (Jones et al., 2002). A recent study by Wei et al. (2003) suggests that even the boundary layers of MCs have their own structure. The inner (closest to the MC) boundary of the layer shows a so called 'triple-low state' (low proton temperature and density, and low plasma beta). However, the outer layer shows the opposite, i.e., a 'triple-high state' (high proton temperature and density, and high plasma beta).

1.3. Magnetic helicity in clouds

One important magnetohydrodynamic (MHD) quantity in MCs is the magnetic helicity (H). H quantifies several aspects of a given magnetic structure, such as the twist, the kink, the number of knots between magnetic field lines, the linking between magnetic flux tubes, etc.

Magnetic helicity is observed in the solar wind on all scales, from more than 1 AU to less than the gyro-radius of a thermal proton (Smith, 2000). In a dynamically turbulent medium, such as the solar wind, magnetic helicity tends to be transported to larger scales (see, e.g., Matthaeus, 2000).

Moreover, H is approximately conserved in the solar atmosphere and the heliosphere (Berger, 1984), and it is very useful to link solar and interplanetary phenomena. When a MC is ejected from the solar corona, it carries an important amount of H. Thus, estimations of the content of H in MCs can help us to understand the physical processes involved in the expulsion of twisted magnetic flux tubes from the Sun and their dynamical evolution in the solar wind. In spite of its relevance, the magnetic helicity contained in solar ejecta, such as interplanetary flux tubes, is poorly known.

There is observational evidence showing that the helicity sign in magnetic clouds matches with their source regions (see, e.g., Bothmer and Schwenn, 1994; Rust, 1994; Marubashi, 1997; Yurchyshyn et al., 2001). To estimate the amount of helicity both in MCs and in the corona, it is necessary to build a magnetic model to fit the available data (since in both cases, the data provide only partial information on the magnetic configuration). For example, a significant fraction of coronal sigmoids (S-shaped magnetic structures) are created by projection effects or magnetic complexity, e.g., Glover et al. (2000), see also Fletcher et al. (2001) for a well studied case; then, the shape of these sigmoids does not contain fully reliable information on the helicity sign and, of course, not on its value.

In the frame of ideal MHD, when the inertial term in the Navier–Stokes equation can be neglected (compared to the magnetic tension, and magnetic and plasma pressure) there is not net force applied on any fluid element. MCs are astrophysical objects to which this approach can be applied, when they are described in the solar wind frame. Then, their magnetic configuration results from the solution of $\vec{\mathbf{J}} \times \vec{\mathbf{B}}/c - \nabla p = 0$, where c is the speed of the light, $\vec{\mathbf{J}} = (c/4\pi)\nabla \times \vec{\mathbf{B}}$ is the electric current, and p is the total plasma pressure.

When the plasma pressure is negligible compared to the magnetic pressure, the configuration is called 'force-free', because the self-force of the magnetic field is null, and the magnetic pressure is balanced by the tension of the curved magnetic field lines.

Taylor (1974) conjectured that in a magnetofluid with 'low resistivity' (and not necessarily null resistivity), confined to a volume bounded by perfectly conducting walls, H can be considered as constant. Thus, the system will relax to a (meta-stable) constant α force-free configuration (i.e., a configuration such that $\nabla \times \mathbf{B} = \alpha \mathbf{B}$), the state of minimum energy keeping H constant, according to the Woltjer's theorem, where the resistivity is exactly zero. However, observations show that the total plasma (thermal) pressure is small but not zero inside MCs, and it is not known how close to force-free is the magnetic configuration.

1.4. Magnetic cloud models

Interplanetary flux tubes or flux ropes (in particular MCs) can be modeled locally using helical cylindrical geometry as a first approximation (Farrugia et al., 1995), using different approaches: a linear force-free field (e.g., Burlaga et al., 1981; Burlaga, 1988; Lepping et al., 1990), a force-free uniformly twisted field (e.g., Farrugia et al., 1999) or even non-force-free models. In particular, four non-force-free models have been recently applied to interplanetary flux tubes: (i) a non-axially symmetric

model (Hu and Sonnerup, 2001), and three axially symmetric models: (ii) with a radial exponential dependency for the azimuthal and poloidal components of the magnetic field (Mulligan and Russell, 2001), (iii) with a constant current density (Hidalgo et al., 2002a), and (iv) with an azimuthal current density depending linearly on the distance to the axis of the tube (Cid et al., 2002). All these models are physically different and it is not yet clear which of them gives the best representation of interplanetary flux tubes. Each author usually uses a given model, but a comparison between the predictions of these various approaches has not yet been done.

MHD simulations of the dynamical evolution of MCs show that propagating flux ropes will have oblate shapes, due to the interaction between the MC and the solar wind (Vandas et al., 1995; Riley et al., 2003). The solar wind background can distort the hypothetical cylindrical initial cross-section of the cloud, producing an elliptical section. Elliptical models have been recently proposed: (i) with a linear force-free field (Vandas and Romashets, 2003) and (ii) non-force free field (Hidalgo et al., 2002b).

For two dimensional systems (i.e., one ignorable coordinate), a useful equation known as 'Grad–Shafranov' can be used to find static solutions (see, e.g., Freidberg, 1987; Biskamp, 1997). The magnetic structure of MCs has been reconstructed from numerical solutions of this equation, using magnetic and pressure observations by Hu and Sonnerup (2002). They found deviations from axial symmetry in the cross-section of the flux rope for two clouds, and they also determined quantitative features, such as the impact parameter, size, chirality, maximum field, and twist of the field lines.

MCs are expanding objects. Moreover, at 1 AU some MCs change significantly their sizes in the Earth–Sun direction during the time scale in which one spacecraft, fixed at 1 AU, observes them. This increasing size can be observed from the large scale trend in the observed bulk speed profile. A MC in expansion corresponds to observations of faster speed when the spacecraft crosses the front of the cloud and slower speed when crossing its rear part.

An ideal MHD self-similar expansion model for the time evolution of clouds has been proposed by Farrugia et al. (1993). From this model, it is possible to predict the expansion velocity and the decrease of the magnetic field. Some works have included expansion effects in their analysis of MCs (e.g., Marubashi, 1997; Osherovich and Burlaga, 1997; Mulligan and Russell, 2001; Hidalgo, 2003).

1.5. Road map of the paper

As in the solar corona, a magnetic model is also needed in the interplanetary space to accurately recover the global magnetic field structure from one dimensional data. One purpose of the present paper is to review some previous results that compare various approaches, which have been proposed for the magnetic configuration in MCs.

In Section 2, we review the concepts of magnetic flux, frozen-in field, and magnetic helicity. Then, in Section 3, we present four cylindrical models to describe the magnetic structure of MCs, giving analytical expressions for the flux and helicity for each of the models. A method to analyze in situ magnetic observations of MCs is presented in Section 4. The analysis of several clouds is presented in Section 5. Finally, in Section 6, we present a discussion of our results and the conclusions.

2. Magnetic flux and helicity

In this section, we briefly review the computation of magnetic magnitudes of interest, such as magnetic flux and helicity, in the classical MHD framework.

The magnetic flux across an arbitrary surface $S(t)$, moving with the fluid is given by

$$F = \int_{S(t)} \vec{\mathbf{B}} \cdot \mathrm{d}\vec{\mathbf{S}}. \tag{1}$$

From Gauss theorem and from $\nabla \cdot \vec{\mathbf{B}} = 0$ it is trivial to show that, at a fixed time t, the magnetic flux across a closed surface around a volume V, $S(V)$, is null (i.e., $F = 0$). Thus, for magnetic flux tubes, the in-flux is equal to the out-flux.

For an ideal magnetofluid, i.e., a fluid with zero resistivity, the induction equation (see, e.g., Sturrock (1994) for details on the complete induction equation) can be generally approximated as

$$\partial_t \vec{\mathbf{B}} = \nabla \times (\vec{\mathbf{v}} \times \vec{\mathbf{B}}), \tag{2}$$

where $\vec{\mathbf{v}}$ is the velocity field of the fluid. From Eqs. (1) and (2), it can be shown (see, e.g., Biskamp, 1997) that the flux on a surface moving with the fluid (the so-called material surface) remains constant $\mathrm{d}F/\mathrm{d}t = 0$. Thus, analyzing the conservation of F on a flux tube of infinitesimal diameter, it is possible to get an image of the so called 'frozen-in' concept, i.e. the magnetic field lines can only be moved together with the fluid.

The magnetic helicity (H) of a field $\vec{\mathbf{B}}$ within a volume V is defined by $H = \int_V \vec{\mathbf{A}} \cdot \vec{\mathbf{B}}\, \mathrm{d}V$, where the vector potential $\vec{\mathbf{A}}$ satisfies $\vec{\mathbf{B}} = \vec{\nabla} \times \vec{\mathbf{A}}$. However, because of the gauge degeneracy of $\vec{\mathbf{A}}$, this definition is physically meaningful only when the magnetic field is fully contained inside the volume V (i.e., at any point of the surface S surrounding V, the normal component $B_\mathrm{n} = \vec{\mathbf{B}} \cdot \hat{\mathbf{n}}$ vanishes).

H is an ideal invariant in three dimensional MHD. When the resistivity is very small but not zero, it decays more slowly than the energy. In a volume V such that

$B_n = 0$, the decay of H is given by (see, e.g., Biskamp, 1997)

$$\frac{dH}{dt} = -\eta \int_V dV \vec{J} \cdot \vec{B}. \quad (3)$$

2.1. Relative magnetic helicity

A gauge-independent relative magnetic helicity H_r can be defined inside a closed volume in three dimensions (Berger and Field, 1984). This relative helicity is obtained by subtracting the helicity of a reference field $\vec{B}_{ref}$ having the same distribution of B_n on S:

$$H_r = H - \int_V \vec{A}_{ref} \cdot \vec{B}_{ref} \, dV. \quad (4)$$

If we choose a different gauge to define the vector potential (i.e., we define $\vec{A}' = A + \vec{\nabla}\psi$, where ψ is any scalar function), the new relative helicity H'_r will be given by:

$$H'_r = H_r - \int \int_{S(V)} \psi(\vec{B} - \vec{B}_{ref}) \cdot \vec{ds} = H_r. \quad (5)$$

Thus, even for cases where $B_n \neq 0$ (as can happen on the legs of interplanetary flux tubes), we can define H_r, which is gauge-invariant.

Several authors have modeled the local magnetic field of an interplanetary flux tube as a straight cylindrical structure with a 2-component magnetic field $\vec{B}(\vec{r}) = B_\varphi(r)\hat{\varphi} + B_z(r)\hat{z}$ (e.g., Burlaga, 1988; Lepping et al., 1990; Farrugia et al., 1995; Hidalgo et al., 2000, 2002a). In this case, the reference field can be chosen as $\vec{B}_{ref}(r) = B_z(r)\hat{z}$ (with null magnetic helicity, since field lines are straight).

Using the condition $\vec{A} \times \hat{n} = \vec{A}_{ref} \times \hat{n}$ at the surface of the cylinder, H_r per unit length (L) can be expressed independently of $\vec{A}_{ref}$ and $\vec{B}_{ref}$ as

$$H_r/L = 2\pi \int_0^R [B_z A_z + A_\varphi B_\varphi - A_{0,z} B_{0,z}] r \, dr = 4\pi \int_0^R A_\varphi B_\varphi r \, dr, \quad (6)$$

where R is the radius of the tube.

3. Cylindrical models for magnetic clouds

Several models have been used to describe the magnetic configuration of MCs. In this section, we will review four different static cylindrical models, force free and non-force free configurations.

3.1. Linear force-free field

The axially symmetric magnetic field of a linear force-free configuration ($\vec{\nabla} \times \vec{B} = \alpha \vec{B}$, with α constant) was obtained by Lundquist (1950). It has been shown that this solution is consistent with in situ measurements of interplanetary magnetic flux tubes at 1 AU (e.g., Burlaga et al., 1981; Burlaga, 1988; Lepping et al., 1990). Thus, the field is well modeled by

$$\vec{B}_L = B_0 J_1(\alpha r)\hat{\varphi} + B_0 J_0(\alpha r)\hat{z}, \quad (7)$$

where J_n is the Bessel function of the first kind of order n, and B_0 is the strength of the field at the MC axis. The magnetic twist per unit length,

$$\tau = d\varphi/dz = B_\varphi/(rB_z), \quad (8)$$

is

$$\tau_L(r) = \frac{J_1(\alpha r)}{r J_0(\alpha r)}. \quad (9)$$

The constant α determines the twist at the flux tube axis, $\tau_{0,L} = \tau_L(0) = \alpha/2$.

The flux F in this model is given by

$$F_L = \frac{2\pi B_0}{\alpha^2} \int_0^{\alpha R} x J_0(x) \, dx. \quad (10)$$

It has been shown that the Lundquist's solution extending to the first zero of J_0 is enough to describe some magnetic clouds (e.g., Lepping et al., 1990). In these cases $F_L \sim 1.4 B_0 R^2$. However, Vandas and Geranios (2001) showed that there are some MCs that seem to be better described using the Lundquist's solution beyond the first zero of J_0.

We obtain the relative helicity per unit length for this force-free field from Eq. (6), taking $\vec{A} = \vec{B}/\alpha$:

$$\frac{H_{r,L}}{L} = \frac{4\pi B_0^2}{\alpha} \int_0^R J_1^2(\alpha r) r \, dr = \left(\frac{8\pi}{U^4} \int_0^U J_1^2(u) u \, du\right) B_0^2 R^4 \tau_{0,L}, \quad (11)$$

where $u = 2\tau_{0,L} r$ and $U = 2\tau_{0,L} R$ are dimensionless quantities. When the boundary of the cloud is such that $\alpha R \sim 2.405$, i.e., the first zero of J_0, $H_{r,L}/L \sim 0.7 B_0 R^3$ (Démoulin et al., 2002). In the last term of Eq. (11), we have rewritten $H_{r,L}/L$ to emphasize that it has the units of the square of the magnetic flux ($(B_0 R^2)^2$) multiplied by a twist per unit length ($\tau_{0,L}$).

3.2. Uniformly twisted field

The non-linear force-free field with a uniform twist has been used to model interplanetary flux tubes (e.g., Farrugia et al., 1999). For this configuration, $\vec{B}$ is given by (Gold and Hoyle, 1960):

$$\vec{B}_{GH} = \frac{B_0 b r}{1 + b^2 r^2}\hat{\varphi} + \frac{B_0}{1 + b^2 r^2}\hat{z}. \quad (12)$$

In this magnetic configuration, the amount by which a given line is twisted is independent of r,

$$\tau_{\mathrm{GH}}(r) = \tau_{0,\mathrm{GH}} = b. \tag{13}$$

The flux in this model is given by

$$F_{\mathrm{GH}} = B_0\pi \ln(1 + b^2R^2)/b^2. \tag{14}$$

From Eq. (6) and

$$\vec{\mathbf{A}}_{\mathrm{GH}} = \frac{B_0}{2b^2 r}\ln(1 + b^2r^2)\hat{\varphi} - \frac{B_0}{2b}\ln(1 + b^2r^2)\hat{\mathbf{z}}, \tag{15}$$

the relative helicity turns out to be

$$\frac{H_{r,\mathrm{GH}}}{L} = \frac{\pi B_0^2}{2b^3}[\ln(1 + b^2R^2)]^2 = \left(\frac{8\pi[\ln(1 + U^2/4)]^2}{U^4}\right)B_0^2R^4\tau_{0,\mathrm{GH}}, \tag{16}$$

where $U = 2\tau_{0,\mathrm{GH}}R$ as in the previous model.

3.3. Constant current field

A non-force-free model has been recently proposed by Hidalgo et al. (2000, 2002a) to describe interplanetary flux ropes. This model assumes a constant current density such as $\vec{\mathbf{j}}(\vec{\mathbf{r}}) = j_\varphi\hat{\varphi} + j_z\hat{\mathbf{z}}$, where j_φ and j_z are constants. Thus, the magnetic field of this configuration is obtained from $\vec{\mathbf{J}} = c\nabla \times \vec{\mathbf{B}}/4\pi$ resulting

$$\vec{\mathbf{B}}_{\mathbf{H}} = (2\pi j_z r/c)\hat{\varphi} + B_0(1 - 4\pi j_\varphi r/(cB_0))\hat{\mathbf{z}}, \tag{17}$$

where B_0 is the field at the center of the tube.

The magnetic field lines twist per unit length as a function of the tube radius can be directly obtained from Eq. (8), giving

$$\tau_H(r) = \frac{2\pi j_z}{cB_0}\frac{1}{1 - 4\pi j_\varphi r/(cB_0)}; \tag{18}$$

therefore, as a result, the twist at the tube center is given by $\tau_{0,H} = 2\pi j_z/(cB_0)$. The flux is $F_H = \pi B_0R^2/3[3 - \frac{8\pi j_\varphi R}{cB_0}]$.

From Eq. (6) and

$$\vec{\mathbf{A}}_{\mathbf{H}} = \left(\frac{B_0 r}{2} - \frac{4\pi j_\varphi r^2}{3c}\right)\hat{\varphi} - \frac{B_0}{2}\tau_{0,H}r^2\hat{\mathbf{z}}, \tag{19}$$

the relative helicity results,

$$\frac{H_{r,H}}{L} = 4\pi\tau_{0,H}B_0R^4\left(\frac{B_0}{8} - \frac{4\pi j_\varphi R}{15c}\right). \tag{20}$$

When B_z is zero at the boundary of the cloud, $B_0 = 4\pi j_\varphi R/C$, and the helicity results:

$$\frac{H_{r,H}}{L} = \frac{7\pi}{30}B_0^2R^4\tau_{0,H}. \tag{21}$$

3.4. Linear azimuthal current

A cylindrical magnetic configuration with a current density such as $\vec{\mathbf{j}}(\vec{\mathbf{r}}) = ar\hat{\varphi} + j_z\hat{\mathbf{z}}$, with a and j_z constants, has been assumed for magnetic clouds by Cid et al. (2002). This structure has a magnetic field distribution given by

$$\vec{\mathbf{B}}_{\mathrm{C}} = 2\pi j_z r/c\hat{\varphi} + B_0(1 - r^2 2\pi a/(cB_0))\hat{\mathbf{z}} \tag{22}$$

and the flux is $F_{\mathrm{C}} = B_0\pi R^2(1 - 2\pi aR^2/(2cB_0))$.

The twist per unit length for this model is given by

$$\tau_{\mathrm{C}}(r) = \frac{2\pi j_z}{cB_0}\frac{1}{1 - \frac{2\pi ar^2}{cB_0}}. \tag{23}$$

While the dependence of the axial twist (τ_0) on j_z and B_z results the same for $\tau_{0,H}$ and $\tau_{0,\mathrm{C}}$ just because both B_φ and B_z at the axis of the cloud are the same for both models, we note a different twist distribution along r for both models.

The vector potential for Cid model is given by

$$\vec{\mathbf{A}}_{\mathrm{C}} = (B_0 r/2 - \pi ar^3/(2c))\hat{\varphi} - 2\pi j_z r^2/(2c)\hat{\mathbf{z}}. \tag{24}$$

Thus, the helicity results:

$$H_{r,\mathrm{C}}/L = \pi^2 j_z B_0 R^4\left(1 - \frac{2\pi aR^2}{3B_0 c}\right)\Big/c. \tag{25}$$

When the axial field is zero at the cloud boundaries, the (maximum) field and the twist at the cloud axis are $B_0 = 2\pi aR^2/c$ and $\tau_{0,\mathrm{C}} = j_z/(aR^2)$, respectively. In this case $F_{\mathrm{C}} = B_0\pi R^2/2$ and $H_{r,\mathrm{C}}/L = \pi\tau_{0,\mathrm{C}}B_0^2R^4/3$.

In our analysis of MCs given in Section 5, we will consider that B_z is zero at the boundary of the cloud when we use the models of Hidalgo et al. and Cid et al., in order to compare the four models, keeping only two degrees of freedom for each model (B_0 and τ_0) when the radius is fixed.

We want to stress that the twist distribution in the flux tube is strongly model dependent (compare Eqs. (9), (13), (18), and (23)). This implies that the obtained values for τ_0, a local quantity, are not directly comparable between different models. A pertinent comparison can only be done with a global quantity, such as the magnetic helicity.

4. Data analysis – in situ measurements

When modeling a MC, we need to define a local system of coordinates linked to the cloud. Assuming that the MC has a cylindrical helical magnetic structure, the natural coordinates to describe its magnetic field are the polar ones (r, φ, z), such that $\vec{B}(r) = B_z(r)\hat{z} + B_\varphi(r)\hat{\varphi}$. When the spacecraft trajectory crosses the axis of the helix (i.e., when the impact parameter p is zero), we can define a cartesian system of coordinates, such that $\hat{z}_{\mathrm{cloud}}$ is parallel to the axis of the cloud and $B_{z,\mathrm{cloud}}$ at this axis is positive. We define also $\hat{x}_{\mathrm{cloud}} = \hat{r}$ when the spacecraft leaves the cloud (i.e., $\hat{x}_{\mathrm{cloud}}$ is equal to the outbound $\hat{r}$), and $\hat{y}_{\mathrm{cloud}}$ is such that the system is right-handed (and so, $\hat{y}_{\mathrm{cloud}}$ is the outbound $\hat{\varphi}$).

To determine the size of a given MC, we need to identity the boundaries of the cloud and the orientation of its axis.

The boundaries can be identified from the observations using several criteria (see Section 1.2). Once the boundaries of a given MC have been identified, it is possible to determine the time when the spacecraft starts (t_s) and ends (t_e) observing the cloud. Thus, we analyze the magnetic properties of several MCs from the time series $\vec{\mathbf{B}}(t)$, for $t_s < t < t_e$.

4.1. Minimum variance

In situ measurements of the magnetic field are provided along a linear cut of the cloud, which results from the trajectory of the spacecraft. We analyze the three components of the magnetic field vector given in GSE coordinates (Geocentric Solar Ecliptic coordinates). In this system of coordinates, $\hat{x}_{GSE}$ corresponds to the Earth–Sun direction, $\hat{z}_{GSE}$ points to the north, perpendicular to the ecliptic plane, and $\hat{y}_{GSE}$ is such that the system is right handed.

When the spacecraft path intersects the axis of an ideal cloud as defined in Section 3 (i.e., the impact parameter, p, is zero), the component $\hat{\varphi}$ of the spacecraft vector trajectory ($\vec{r}_s$) will be zero (i.e., $\vec{r}_s(t) = \alpha(t)\hat{r} + \beta(t)\hat{z}$). Thus, in this case, the magnetic field data obtained by the spacecraft will show: $B_{x,\,\mathrm{cloud}} = 0$, a large and coherent variation of $B_{y,\,\mathrm{cloud}}$ (with a change of sign), and an intermediate and coherent variation of $B_{z,\,\mathrm{cloud}}$, from low values at one cloud edge, taking the largest value at its axis and returning to low values at the other edge (e.g., Bothmer and Schwenn, 1994).

It is possible to estimate the orientation of a magnetic cloud applying the minimum variance (MV) method to the magnetic observations (Sonnerup and Cahill, 1967). This method finds the direction ($\hat{\mathbf{n}}$) in which the mean quadratic deviation of the field, $\langle(\mathbf{B}\cdot\hat{\mathbf{n}} - \langle\mathbf{B}\cdot\hat{\mathbf{n}}\rangle)^2\rangle$, is minimum (maximum). It is possible to show that this is equivalent to finding the eigenvector corresponding to the smallest (highest) eigenvalue of the covariance matrix $M_{i,j} = \langle B_i B_j\rangle - \langle B_i\rangle\langle B_j\rangle$. Thus, this MV method determines the direction of the maximum ($\hat{\mathbf{y}}_{\mathrm{cloud}}$), intermediate ($\hat{\mathbf{z}}_{\mathrm{cloud}}$), and minimum ($\hat{\mathbf{x}}_{\mathrm{cloud}}$) variance of the field, and so determines the orientation of the MC axis. A more complete discussion of the MV method applied to interplanetary flux tubes can be found in the appendix of Bothmer and Schwenn (1998).

4.2. Fitting of physical parameters

From the application of the MV method to the time series of the magnetic field components inside the cloud, we find the orientation of the cloud. Then, from the obtained eigenvectors, we construct a rotation matrix and obtain the components of the observed magnetic field in the 'cloud' coordinates: $B_{x,\,\mathrm{cloud}}$, $B_{y,\,\mathrm{cloud}}$, $B_{z,\,\mathrm{cloud}}$.

From the observed bulk velocity of the interplanetary plasma and from the orientation of the cloud axis, we estimate the radius of the cloud. We also associate each observed time (t_i) with the corresponding distance from the craft to the cloud axis (r_i), getting the magnetic field inside the cloud as a function of the radius, i.e., $\vec{B}_{\mathrm{obs}}(r)$.

We define a residual function (χ^2), comparing $\vec{B}_{\mathrm{obs}}(r)$ with $\vec{B}_{\mathrm{model}}(r)$ for each of the models described in Sections 3, such that in the 'cloud' coordinates it is given by

$$\chi^2 = \sum_{i=1}^{N}\Big[(B^i_{x,\mathrm{obs}} - B^i_{x,\mathrm{model}})^2 + (B^i_{y,\mathrm{obs}} - B^i_{y,\mathrm{model}})^2 + (B^i_{z,\mathrm{obs}} - B^i_{z,\mathrm{model}})^2\Big]. \quad (26)$$

We minimize χ^2 through the standard non-linear least-square fitting Levenberg–Marquardt routine (Press et al., 1992), fitting the free parameters of the models (e.g., B_0 and τ_0).

5. Flux and helicity from observations

From the expressions for H and F for the four models described in Section 3, and after fitting the free parameters for each model, we compare the values of these magnitudes for several interplanetary flux ropes in the next sections.

First (Section 5.1), we present average values of H from previous statistical studies under the linear force free model. Then (Sections 5.2–5.5), we present the analysis of our results on several interplanetary coronal mass ejections, following the method described in Section 4. We quantify F and H, and we analyze their sensitivity when different models are assumed. First, we analyze a well known magnetic cloud observed by the spacecraft Wind on October 18–19, 1995 (see e.g. Lepping et al., 1997; Larson et al., 1997). Then, we study a very small magnetic cloud, observed by Wind on May 15–16, 1998. After that, we analyze a hot interplanetary flux rope, which is not classified as a magnetic cloud, only because its temperature is not low, but it presents a large scale coherent rotation, and high magnetic field. Finally, we present statistical results of the sensitivity of F and H to the different models.

5.1. Previous statistical analysis

The magnetic field of 18 MCs has been analyzed by Lepping et al. (1990). They found an average magnetic intensity at the axis of the cloud of $B_0 = (20 \pm 7)$ nT and an average radius of $R = (0.14 \pm 0.05)$ AU, under the assumption of a linear force-free cylindrical model for the clouds.

Other statistical study has been done by Zhao et al. (2001). They analyzed 23 cases and found that $B_0 = (24 \pm 8)$ nT and $R = (0.11 \pm 0.05)$ AU.

From the average values obtained from the statistical studies made by Lepping et al. (1990) and Zhao et al. (2001), assuming a cylindrical linear force-free magnetic configuration, and an axial length for the cloud of ~0.5 AU, Green et al. (2002) estimated the average magnetic helicity in clouds as $H \sim 2 \times 10^{42}$ Mx^2.

5.2. October 18–19, 1995

The plasma and magnetic data obtained by Wind indicate that the cloud started to cross the spacecraft at ~19 UT, on October 18, 1995 (Lepping et al., 1997). While the beginning of the cloud is very clear, its end time is controversial. Several authors (e.g., Lepping et al., 1997; Janoo et al., 1998; Collier et al., 2001) have taken it as ~23 UT, on October 19, 1995, which is the end time chosen by us. The orientation, the diameter, and the physical parameters have been determined for this cloud by Lepping et al. (1997) under the assumption of a linear force-free field model, and by Hidalgo et al. (2002a) under the assumption of a non-force-free constant current model.

Collier et al. (2001) found that while Wind crossed this MC, the magnetic field lines show signatures of connectivity to the Sun in both ends in some parts, only in one extreme in others, and even disconnection in others. The length of the magnetic field lines at the center of the cloud, when at least one of their ends was connected to the Sun, has been estimated from in situ observations (at 1 AU) of impulsive electron events (~1–10^2 keV) and solar type III radio bursts produced by these electrons near the Sun (Larson et al., 1997). From an analysis of the arrival time of these electrons, the semi-length of these field lines, which agrees with the semi-length of the cloud axis, has been estimated as ~1.2 AU.

Fig. 2 shows the components of the field in the cloud frame, as resulted from the application of the MV method (see Section 4.1). Note the largest scale variance of $B_{y,\mathrm{cloud}}$ (middle panel), medium of $B_{z,\mathrm{cloud}}$ (left panel), and lowest of $B_{x,\mathrm{cloud}}$ (right panel).

The observed field (B_z and B_y components, in the cloud frame) together with the plots of the fitted Lundquist model are presented in Fig. 3.

We fit the free parameters of the cylindrical linear force-free field model from the observations of this cloud, as described in Section 4. From the fitted parameters ($B_0 = 24.3$ nT and $\tau_{0,L} = 10.0$ AU^{-1}), we compute F and H_r, obtaining $F = 1.1 \times 10^{21}$ Mx, and $H_r = +9.4 \times 10^{42}$ Mx^2, assuming a length for the cloud axis of 2.4 AU, according with Larson et al. (1997).

The solar source of this MC was located in the Active Region (AR) NOAA 7912 (van Driel-Gesztelyi et al., 2000). The coronal field before and after the ejection have been modeled, extrapolating the observed photospheric line of sight component of the field, under the linear (or constant α) force-free field assumption: $\vec{\nabla} \times \vec{B} = \alpha \vec{B}$ (see, e.g., Alissandrakis, 1981; Mandrini et al., 1996; Démoulin et al., 1997). The photospheric line of sight magnetograms are used as boundary conditions and the value of α is determined by fitting the computed field lines to the observed X-ray loops. Luoni et al. (2005) estimated the variation of the coronal helicity, before and after the ejection of this cloud. The obtained value was $\Delta H \sim +4.5 \times 10^{42}$ Mx^2, a similar value to that estimated from the cloud. Thus, a good agreement was found between the ejection of coronal helicity and the interplanetary H contained in this MC.

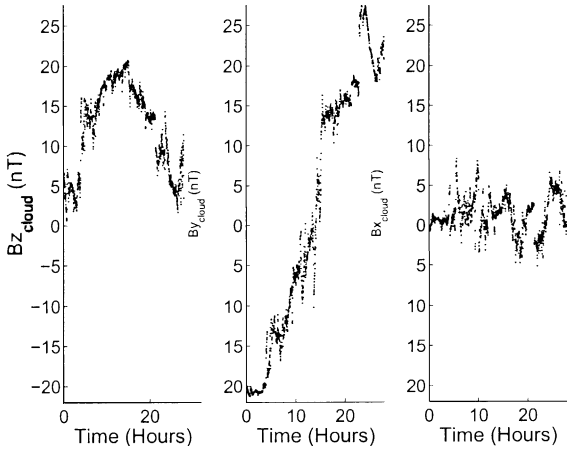

Fig. 2. Magnetic field for the cloud of October, 1995, in the cloud coordinates (see main text for details). Time corresponds to hours after 19:00 UT of October 18, 1995.

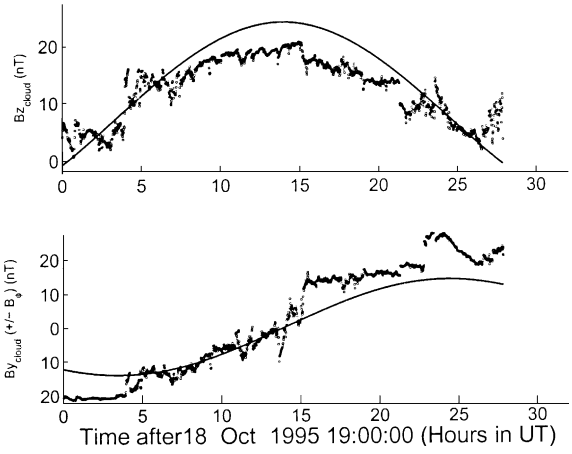

Fig. 3. Data (big dots) and curves from the Lundquist model (thin continuous curve) for B_z and B_y components (cloud frame).

5.3. Small magnetic cloud

We analyze here a small MC, which was linked with its coronal source by Mandrini et al. (2005). The cloud

was observed by Wind between 22:00 UT, on May 15 of 1998, and 01:50 UT on May 16 (a duration of ~4 h), and its solar source was identified as a small active region, that presented signatures of erupting material at 8:30 UT on May 11, 1998.

The coherent rotation of the magnetic field vector is shown in Fig. 4 after a MV analysis. With this approach, the spacecraft impact parameter, p, is not determined and we set it equal to zero. Note that the large angle rotation of the field (~147°, see left panel of Fig. 4) indicates that the ratio between the impact parameter and the radius of the cloud (p/R) should be small. This field rotation also implies that the sign of the helicity is negative. We estimate its radius as $R \sim 1.6 \times 10^{-2}$ AU, which implies a very small MC (~10 times smaller than average).

We fit the Lundquist, Gold–Hoyle, and Hidalgo et al. models to the observed field components. in the cloud coordinates (see Section 4.2) The two panels in Fig. 5 correspond to $B_{z,\mathrm{cloud}}$ and $B_{y,\mathrm{cloud}}$ for the small MC. The observed data are shown with thick lines and the curves obtained using the parameters fitted to the Lundquist model are shown with thin lines. The other two models produce similar curves.

From the different models, we obtain similar values for B_0 (~13.8–15.9 nT). The twist of the field lines near the center of the tube ($|\tau_0| = 51$–$85\ \mathrm{AU}^{-1}$) is lower for the Hidalgo et al. model and larger (by ~70% respect to the lower value) for the Gold–Hoyle model (see details in Mandrini et al., 2005).

The magnetic flux (F) of B_z (i.e., along the flux tube) shows a narrow range in the force-free cases, $F \sim 1.3$–1.4×10^{19} Mx, but it changes by ~−30% for the Hidalgo model. The magnetic flux for this small magnetic cloud is about one hundredth of the average value for magnetic clouds, $F \sim 10^{21}$ Mx (Green et al., 2002).

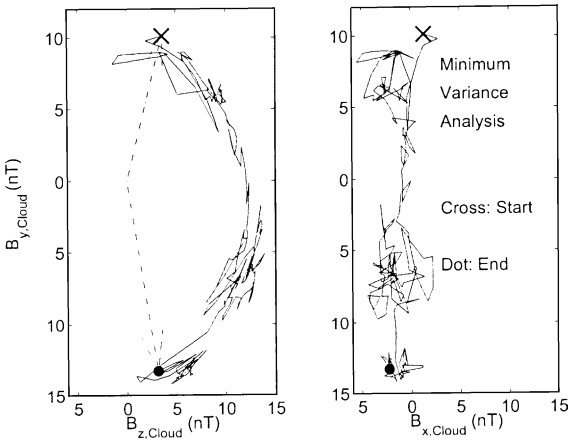

Fig. 4. The two panels show the hodograms for the small MC of May, 1998. The left panel shows the coherent rotation, while the right panel shows the noise in the $\hat{x}_{\mathrm{cloud}}$ direction.

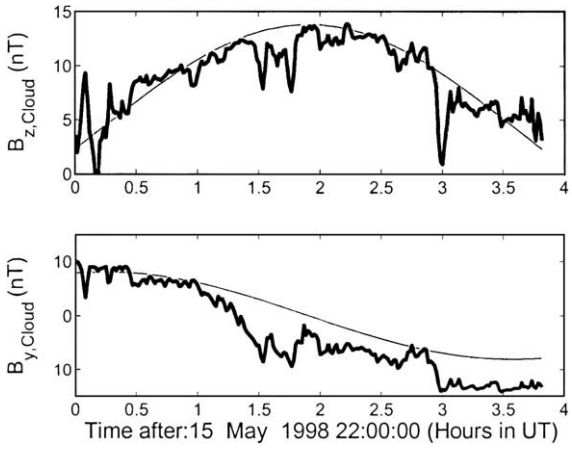

Fig. 5. Magnetic field components in cloud coordinates for the cloud of May, 1998. The panels show the evolution of the magnetic field components (see text). The observed magnetic data are drawn with thick lines, and the best solution fitted using Lundquist model is shown with thin lines.

The helical magnetic field of the flux tube is left-handed so H_r is negative and it is in the range $|H_r|/L \sim (2.8$–$3) \times 10^{39}$ Mx^2/AU for the three models, a very small interval. The magnetic helicity per unit length for this event is smaller than for typical clouds by three orders of magnitude (Green et al., 2002).

The coronal field is computed as in the previous Section. To compute the model and its free parameter (α), we have used magnetograms from MDI (Michelson Doppler Imager, Scherrer et al., 1995), on board the Solar and Heliospheric Observatory, SoHO) as boundary conditions, and the coronal loops observed with the Transition Region and Coronal Explorer (TRACE, Handy et al., 1999).

From the fit, we obtain $\alpha < 0$ and, therefore, the helicity of this coronal configuration is negative. The coronal magnetic helicity before and after the ejection was computed, giving a negative difference such as $|\Delta H_{\mathrm{cor}}| \sim 2$–$3 \times 10^{39}$ Mx^2.

For the comparison of the coronal and interplanetary magnetic helicities, one of the main unknowns is the distribution of the twist along the flux rope. Even assuming a given distribution of the twist, the MC length is unknown. In large-scale MCs, there is often evidence that they are still connected to the Sun when they are observed at 1 AU (e.g., presence of bi-streaming electrons). This leads to a MC length slightly larger than 2 AU. However, for this small MC, the photospheric magnetic bipole disappeared about one day after the eruption (Mandrini et al., 2005), so the erupting flux rope was well detached from its original solar source when it was observed in situ ≈4.5 days after the coronal eruption. A simple proportionality gives a length of ≈0.5 AU. However, after reconnection with large-scale field lines, the magnetic twist contained in the ejected

flux tube propagates along the new connections as a torsional Alfvén wave. Taking a typical Alfvén velocity of 100 km s^{-1}, the twist can propagate on both sides of the flux tube over a length of 0.2 AU in 3.5 days. We conclude that the probable length of the observed MC is between 0.5 and 1 AU.

Thus, the estimated cloud helicity is, $|H_{cloud}| \approx 1.5$–3×10^{39} Mx^2, very close to the observed values found at the coronal level ($|\Delta H_{cor}| = 2$–3×10^{39} Mx^2). So, as in the previous analyzed cloud, we obtain a good agreement between the coronal and interplanetary helicities.

5.4. Hot flux tube

We analyze here the magnetic configuration of a flux tube observed by Wind on October 24–25, 1995 (see Fig. 1 of Farrugia et al., 1999). This flux tube presents a large and smooth rotation of the field (see Fig. 1 of Dasso et al., 2003c) and a low value of the proton plasma beta ($\beta_p \sim 0.2$–0.4), similar to what can be observed in some MCs (see, e.g., Dasso et al., 2001). However, near the center of the tube (at around 50% of its size) T_p was a factor $\sim$10 higher than near its boundaries and, thus, it is not classified as a MC but rather as a "hot flux tube". However, the value of β_p remains low because the higher temperature region has a lower density. The total β (including the contribution of electron and alpha particles to the pressure) is in the range 0.8–1.0 in the whole event. A preliminary analysis of the helicity of this hot tube was done by Dasso et al. (2003b).

We find a well defined orientation for the flux tube axis from MV. We use this orientation to model the observed field, according to Lundquist, Gold–Hoyle, and Hidalgo et al. models, and we obtain the two physical parameters (the twist at the tube center and B_0) that best fit the observations following the method discussed in Dasso et al. (2003b,c).

In order to test the validity of the MV method, and to determine the impact parameter, we have also simultaneously fitted (SF) the geometrical parameters (the orientation angles), the impact parameter (p) and the two physical parameters (B_0 and τ_0) for each of the three models. The SF was done (for each model) using the observed field in GSE (as described in Hidalgo et al., 2002a). The least-square fitting for the SF has been also done using the standard Levenberg–Marquardt routine (Press et al., 1992).

The radius of the flux tube was estimated as $R \sim 3$–4×10^{-2} AU, when the three models and MV and SF methods are used. The fitted impact parameter (with SF) was only 8% of R with both force-free models. This result justifies, a posteriori, setting p to zero in the MV method.

The three panels of Fig. 6 depict the GSE components of the measured magnetic field, together with the curves obtained from each model, using the SF method. Curves obtained from MV and fitting of B_0 and the twist at the tube center are very similar for the three models.

From a comparison of the values of $\sqrt{\chi^2}$ using the MV and the SF methods, we find, as expected, that the SF provides a slightly better quality fit than the MV method, for the three models. Both linear force free models yield very similar values for $\sqrt{\chi^2}$ (with only about $\sim$1% difference).

The twist per unit length at the tube center is found to be in the range $\sim$20–40 AU^{-1} showing that the flux tube is significantly twisted along its length (with a typical length of $\sim$1 AU, the central part has between 3 and 6 turns). Comparing the MV and SF methods, we find only $\sim$1% difference on the axial twist for a given force-free model.

The central field strength, B_0, is also well determined; the results are very close with both the MV and SF methods and we find only 4% difference between the two force-free models.The field strength B_0 lies in the interval 7.3–7.6 nT, well above the mean variation around the fit ($\sqrt{\chi^2} \sim 1.3$ nT). The largest variations, $\sim$20%–40%, are obtained for Hidalgo et al. model with both methods.

From the fitted model parameters, we obtained a flux $F \sim 3.0$–3.1×10^{19} Mx for both force-free cases, and $2.2 < F < 3.6 \times 10^{19}$ Mx for Hidalgo et al. model.

H_r is positive and from the force-free models $5.6 \times 10^{39} < H_r/L < 7.1 \times 10^{39}$ Mx^2/AU, while $H_r/L = 5.6 \times 10^{39}$ Mx^2/ AU and $H_r/L = 11.1 \times 10^{39}$ Mx^2/AU for the constant current model, using MV and SF fitting, respectively. With the constant current model, the differences found in the parameters (R, B_0) are amplified in the helicity results (since H_r has a non-linear dependence on these parameters, see Eq. (21)).

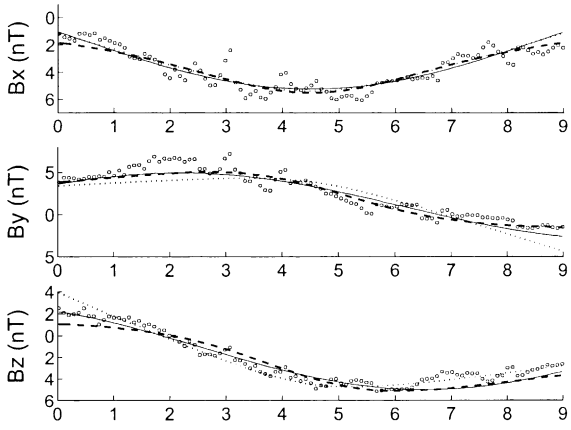

Fig. 6. B_x, B_y, and B_z components of the magnetic field (in Geocentric Solar Ecliptic coordinates, GSE) for the flux tube observed on 24–25 October, 1995. Circles correspond to the observed field (with 5 min averaging), solid line to Lundquist model, dashed to Gold–Hoyle model, and dotted line to Hidalgo et al. model, as arises from a SF method.

5.5. Study of eight well behaved MCs

In this section, we quantify F and H_r/L for a set of eight MCs. We investigate how model-dependent are the results using the four models described in Section 3.

We select those MCs of better quality (quality one) observed by Wind between August 22, 1995 and October 12, 1997, from the web site: http://lepmfi.gsfc.nasa.gov/mfi/mag_cloud_pub1.html. The list of these events, giving the start time (i.e., the time when Wind started to observe the cloud) and the end time, is presented in Table 1.

After applying a MV analysis to the magnetic field vector of each cloud, we fit B_0 and τ_0 for each of the four models, and from the fitting results, we accordingly compute F and H_r/L.

Fig. 7 shows the axial field (B_0) and the radius (R). Fig. 8 (upper panel) shows the magnetic flux F and the magnetic helicity per unit length, H_r/L (lower panel).

In both figures the error bars are computed as the semi-difference between the maximum and minimum values, for the four models. From the error bars of F and H_r/L, we see that for a given cloud, the relative dispersion of H_r/L is much lower than the relative dispersion for F. Therefore, the helicity is more model independent than the flux F.

Figs. 7 and 8 show a general trend to larger values of F and H_r when the radius is larger (a result consistent with the dependence of F and H_r with R, see Section 3). A detailed analysis of F and H_r, and also a study of the magnetic and kinetic energies, is presented by Gulisano et al. (2005) for a more extended set of clouds than the one discussed here.

From Eqs. (7), (12), (17), (22), it is evident that while the component $\hat{\varphi}$ of the magnetic field depends on the two physical free parameters (τ_0 and B_0) in the two force free models, B_φ does not depend on B_0 in both non-force free models. So, while τ_0 and B_0 are coupled in the simultaneous fitting of B_φ and B_z for the force free models, they are uncoupled for the non-force free models. Thus, we prefer to group the models in force free and non-force free to compare their quality. From a visual inspection of the data and the fitted force free models (and also from a χ^2 test), it is not possible to determine which is the best force free model; Lundquist's model or Gold and Hoyle's model can both give relatively good representations for the cloud section. However, from a comparison between the non-force free models, we conclude that Cid's model gives a better representation than Hidalgo's model.

Table 1
List of magnetic clouds (MCs) analyzed in Section 5.5, see main text

#	Start	End
1	22 UT, 22-Aug-1995	19 UT, 23-Aug-1995
2	19 UT, 18-Oct-1995	00 UT, 20-Oct-1995
3	15 UT, 27-May-1996	07 UT, 29-May-1996
4	13 UT, 07-Aug-1996	10 UT, 08-Aug-1996
5	03 UT, 24-Dec-1996	10 UT, 25-Dec-1996
6	05 UT, 10-Jan-1997	02 UT, 11- Jan-1997
7	22 UT, 21-Sep-1997	18 UT, 22-Sep-1997
8	23 UT, 10-Oct-1997	00 UT, 12-Oct-1997

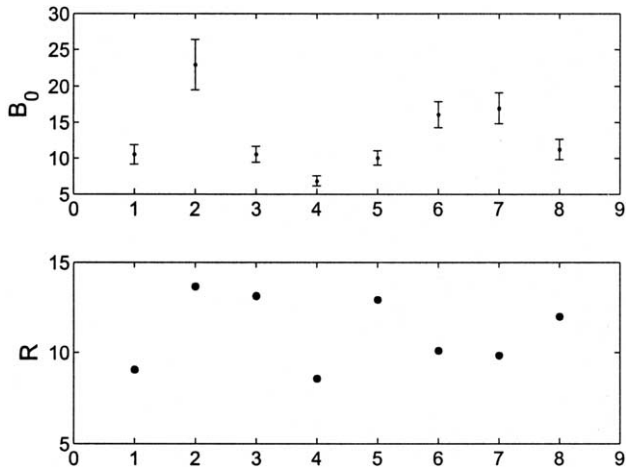

Fig. 7. Axial Field (B_0) in nT (upper panel) and radius in 10^{-2} AU (lower panel) for the eight analyzed MCs. Error bars in B_0 correspond to the semi-difference between the maximum and minimum values obtained from the four models.

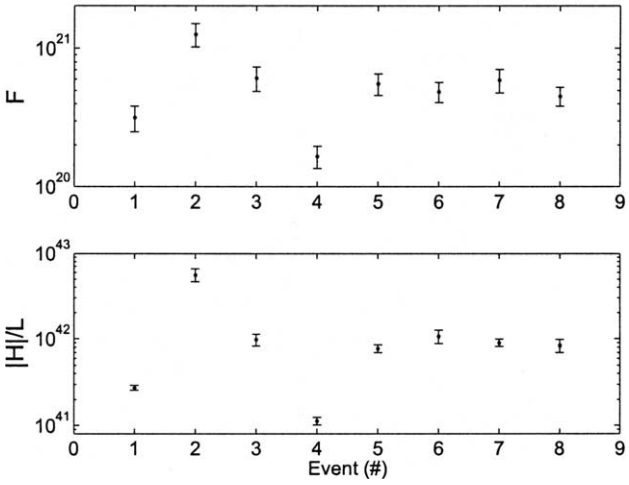

Fig. 8. Flux in Mx (upper panel) and magnetic helicity per unit length in Mx^2/AU (lower panel) for the eight analyzed MCs. Error bars are given as in Fig. 7.

6. Discussion and conclusions

Transient ICMEs have their origin in an instability of the solar coronal field. The magnetic field ejected from the Sun carries the magnetic helicity (H) of its

original field, and since H is not dissipated in the corona nor in the heliosphere, H will be contained in the ICME.

To improve our knowledge of the physical characteristics of magnetic clouds (MCs), and their solar source regions, the quantification of global magnitudes, such as the magnetic flux and helicity, are needed. In particular, they are appropriate to quantify the link between a given MC and its coronal origin.

Both magnetic flux and helicity are very useful quantities, partly because they are conserved, and partly because techniques to measure both coronal values and photospheric fluxes are presently being developed (see e.g., van Driel-Gesztelyi et al., 2003 and references therein). In the interplanetary medium, even though the observations are done 'in situ', these data are insufficient to determine the real three dimensional structure of MCs. However, future observations from the STEREO mission will give valuable hints to determine their configuration.

We reviewed the general properties of ICMEs and MCs, describing four cylindrical models to represent their magnetic configuration at 1 AU. In particular, we derived expressions for the helicity for each model and presented two methods to analyze in situ measurements of MCs.

Two MCs and an interplanetary hot tube were analyzed in detail, quantifying their magnetic flux and helicity. We compared the magnetic helicity contained in the two magnetic clouds, with their solar sources, and found a good agreement between the coronal and the interplanetary helicity values for both events.

We also presented a statistical study of MCs comparing several models. Despite the important variations in the distribution of the twist assumed by the different models, we found that the most relevant magnitude, the magnetic helicity, is almost independent from the cylindrical model used.

An elliptical shape has been suggested for the section of some clouds (e.g., Riley et al., 2003) as consequence of the interaction between the cloud and the solar wind environment. One of our next steps is to compare the quality of the fitting to the observations between these new models and cylindrical ones, which are the most commonly used. Furthermore, we will compute F and H_r and compare the values obtained with the different assumptions. However, it is not possible to certainly determine the exact shape of the cloud from one-spacecraft observations and the knowledge of the section shape will be provided by future stereoscopic observations from the STEREO mission.

More studies of MCs and their coronal counterpart, using not only the helicity sign but also quantifying F and H_r, are needed to improve the current coronal and interplanetary models of CMEs/ICMEs, and also the understanding of the link between them.

Acknowledgments

This research has made use of NASA's Space Physics Data Facility (SPDF). This work was partially supported by the Argentinean grants: UBACyT X329, PIPs 2693 and 2388 (CONICET), and FONCyT (ANPCyT) PICTs O3-12187 and 03-14163. S.D. and C.H.M. are members of the Carrera del Investigador Científico, CONICET. C.H.M. and P.D. thank ECOS (France) and SECyT (Argentina) for their cooperative science program A01U04.

References

Alissandrakis, C.E. On the computation of constant alpha force-free magnetic field. Astron. Astrophys. 100 (July), 197–200, 1981.

Bame, S.J., Asbridge, J.R., Feldman, W.C., Gosling, J.T., Zwickl, R.D. Bidirectional streaming of solar wind electrons greater than 80 eV – ISEE evidence for a closed-field structure within the driver gas of an interplanetary shock. Geophys. Res. Lett. 8 (February), 173–176, 1981.

Baumjohann, W., Treumann, R.A. Basic Space Plasma Physics. Imperial College Press, London, 1996.

Berger, M.A. Rigorous new limits on magnetic helicity dissipation in the solar corona. Geophys. Astrophys. Fluid Dynam. 30 (September), 79–104, 1984.

Berger, M.A., Field, G.B. The topological properties of magnetic helicity. J. Fluid Mech. 147, 133–148, 1984.

Biskamp, D. Non-linear Magnetohydrodynamics. Cambridge University Press, Cambridge, 1997.

Borrini, G., Gosling, J.T., Bame, S.J., Feldman, W.C. Helium abundance enhancements in the solar wind. J. Geophys. Res. 87 (September), 7370–7378, 1982.

Bothmer, V., Schwenn, R. Eruptive prominences as sources of magnetic clouds in the solar wind. Space Sci. Rev. 70 (October), 215–220, 1994.

Bothmer, V., Schwenn, R. The structure and origin of magnetic clouds in the solar wind. Ann. Geophys. 16, 1–24, 1998.

Burlaga, L., Sittler, E., Mariani, F., Schwenn, R. Magnetic loop behind an interplanetary shock – Voyager, Helios, and IMP 8 observations. J. Geophys. Res. 86 (August), 6673–6684, 1981.

Burlaga, L.F. Magnetic clouds and force-free fields with constant alpha. J. Geophys. Res. 93 (July), 7217–7224, 1988.

Burlaga, L.F. Magnetic clouds. in: Schwenn, R., Marsch, E. (Eds.), Physics of the Inner Heliosphere, vol. II. Springer-Verlag, Berlin, pp. 1–22, 1990.

Burlaga, L.F. Interplanetary Magnetohydrodynamics. Oxford University Press, New York, 1995.

Cane, H.V., Richardson, I.G. Interplanetary coronal mass ejections in the near-Earth solar wind during 1996–2002. J. Geophys. Res. 108 (April), 1156, 2003.

Cid, C., Hidalgo, M.A., Nieves-Chinchilla, T., Sequeiros, J., Viñas, A.F. Plasma and magnetic field inside magnetic clouds: a global study. Sol. Phys. 207 (May), 187–198, 2002.

Collier, M.R., Szabo, A., Farrell, W.M., Slavin, J.A., Lepping, R.P., Fitzenreiter, R., Thompson, B., Hamilton, D.C., Gloeckler, G., Ho, G.C., Bochsler, P., Larson, D., Ofman, L. Reconnection remnants in the magnetic cloud of October 18–19, 1995: a shock, monochromatic wave, heat flux dropout, and energetic ion beam. J. Geophys. Res. 106 (August), 15985–16000, 2001.

Dasso, S., Farrugia, C.J., Gratton, F.T., Lepping, R.P., Ogilvie, K.W., Fitzenreiter, R.J. Waves in the proton cyclotron frequency range in

the CME observed by wind on August 7–8, 1996: theory and data. Adv. Space Res. 28, 747–752, 2001.

Dasso, S., Gratton, F.T., Farrugia, C.J. A parametric study of the influence of ion and electron properties on the excitation of electromagnetic ion cyclotron waves in coronal mass ejections. J. Geophys. Res. 108 (April), 1149, 2003a.

Dasso, S., Mandrini, C.H., Démoulin, P. The magnetic helicity of an interplanetary hot flux rope. in: Velli, M., Bruno, R., Malara, F. (Eds.), AIP Conference Proceedings: Solar Wind Ten. American Institute of Physics, New York, pp. 786–789, 2003b.

Dasso, S., Mandrini, C.H., Démoulin, P., Farrugia, C.J. Magnetic helicity analysis of an interplanetary twisted flux tube. J. Geophys. Res. 108 (October), 1362, 2003c.

Démoulin, P., Bagala, L.G., Mandrini, C.H., Henoux, J.C., Rovira, M.G. Quasiseparatrix layers in solar flares II. Observed magnetic configurations. Astron. Astrophys. 325 (September), 305–317, 1997.

Démoulin, P., Mandrini, C.H., van Driel-Gesztelyi, L., Thompson, B.J., Plunkett, S., Kovári, Z., Aulanier, G., Young, A. What is the source of the magnetic helicity shed by CMEs? The long-term helicity budget of AR 7978. Astron. Astrophys. 382 (February), 650–665, 2002.

Farrugia, C.J., Burlaga, L.F., Lepping, R.P. Magnetic clouds and the quiet/storm effect at Earth: A review. in: Tsurutani, B.T., Gonzalez, W., Kamide, Y., Arballo, J. (Eds.), Magnetic Storms, Geophys. Monogr. Ser., vol. 98. American Geophysical Union, Washington, DC, pp. 91–106, 1997.

Farrugia, C.J.., Burlaga, L.F., Osherovich, V.A., Richardson, I.G., Freeman, M.P., Lepping, R.P., Lazarus, A.J. A study of an expanding interplanatary magnetic cloud and its interaction with the earth's magnetosphere – the interplanetary aspect. J. Geophys. Res. 98 (May), 7621–7632, 1993.

Farrugia, C.J., Janoo, L.A., Torbert, R.B., Quinn, J.M., Ogilvie, K.W., Lepping, R.P., Fitzenreiter, R.J., Steinberg, J.T., Lazarus, A.J., Lin, R.P., Larson, D., Dasso, S., Gratton, F.T., Lin, Y., Berdichevsky, D. A uniform-twist magnetic flux rope in the solar wind. in: Habbal, S.R., Esser, R., Hollweg, J., Isenberg, P.A. (Eds.), AIP Conference Proceedings 471: Solar Wind Nine. American Institute of Physics, New York, pp. 745–748, 1999.

Farrugia, C.J., Osherovich, V.A., Burlaga, L.F. Magnetic flux rope versus the sphero-mak as models for interplanetary magnetic clouds. J. Geophys. Res. 100 (July), 12293–12306, 1995.

Farrugia, C.J., Vasquez, B., Richardson, I.G., Torbert, R.B., Burlaga, L.F., Biernat, H.K., Mühlbachler, S., Ogilvie, K.W., Lepping, R.P., Scudder, J.D., Berdichevsky, D.E., Semenov, V.S., Kubyshkin, I.V., Phan, T.-D., Lin, R.P. A reconnection layer associated with a magnetic cloud. Adv. Space Res. 28, 759–764, 2001.

Fletcher, L., López Fuentes, M.C., Mandrini, C.H., Schmieder, B., Démoulin, P., Mason, H.E., Young, P.R., Nitta, N. A relationship between transition region brightenings, abundances, and magnetic topology. Sol. Phys. 203 (November), 255–287, 2001.

Freidberg, J.P. Ideal Magnetohydrodynamics. Plenum Press, New York, 1987.

Galvin, A.B., Ipavich, F.M., Gloeckler, G., Hovestadt, D., Tsurutani, B.T. Solar wind iron charge states preceding a driver plasma. J. Geophys. Res. 92 (November), 12069–12081, 1987.

Glover, A., Ranns, N.D.R., Harra, L.K., Culhane, J.L. The onset and association of CMEs with sigmoidal active regions. Geophys. Res. Lett. 27 (July), 2161–2164, 2000.

Gold, T., Hoyle, F. On the origin of solar flares. Mon. Not. R. Astron. Soc. 120 (January), 89–105, 1960.

Gonzalez, W.D., Tsurutani, B.T., Clúa de Gonzalez, A.L. Interplanetary origin of geomagnetic storms. Space Sci. Rev. 88, 529–562, 1999.

Gosling, J.T. Coronal mass ejections and magnetic flux ropes in interplanetary space. in: Russell, C.T., Priest, E.R., Lee, L.C. (Eds.), Physics of Magnetic Flux Ropes, Geophys. Monogr. Ser., vol. 58. American Geophysical Union, Washington, DC, pp. 343–364, 1990.

Gosling, J.T. Coronal mass ejections: An overview. in: Crooker, N., Joselyn, J.A., Feynman, J. (Eds.), Coronal Mass Ejections, Geophysical Monograph, vol. 99. American Geophysical Union, Washington, DC, pp. 9–16, 1997.

Gosling, J.T., Asbridge, J.R., Bame, S.J., Feldman, W.C., Zwickl, R.D., Paschmann, G., Sckopke, N., Hynds, R.J. Interplanetary ions during an energetic storm particle event – the distribution function from solar wind thermal energies to 1.6 MeV. J. Geophys. Res. 86 (February), 547–554, 1981.

Gosling, J.T., Baker, D.N., Bame, S.J., Feldman, W.C., Zwickl, R.D., Smith, E.J. Bidirectional solar wind electron heat flux events. J. Geophys. Res. 92 (August), 8519–8535, 1987.

Green, L.M., López fuentes, M.C., Mandrini, C.H., Démoulin, P., van Driel-Gesztelyi, L., Culhane, J.L. The magnetic helicity budget of a cme-prolific active region. Sol. Phys. 208 (July), 43–68, 2002.

Gulisano, A., Dasso, S., Mandrini, C.H., Demoulin, P. Global magnetohydrodynamic magnitudes of magnetic clouds. J. Atmos. Sol–Terr. Phys., 2005 (in press).

Handy, B.N., Acton, L.W., Kankelborg, C.C., Wolfson, C.J., Akin, D.J., Bruner, M.E., Caravalho, R., Catura, R.C., Chevalier, R., Duncan, D.W., Edwards, C.G., Feinstein, C.N., Freeland, S.L., Friedlaender, F.M., Hoffmann, C.H., Hurlburt, N.E., Jurcevich, B.K., Katz, N.L., Kelly, G.A., Lemen, J.R., Levay, M., Lindgren, R.W., Mathur, D.P., Meyer, S.B., Morrison, S.J., Morrison, M.D., Nightingale, R.W., Pope, T.P., Rehse, R.A., Schrijver, C.J., Shine, R.A., Shing, L., Strong, K.T., Tarbell, T.D., Title, A.M., Torgerson, D.D., Golub, L., Bookbinder, J.A., Caldwell, D., Cheimets, P.N., Davis, W.N., Deluca, E.E., McMullen, R.A., Warren, H.P., Amato, D., Fisher, R., Maldonado, H., Parkinson, C. The transition region and coronal explorer. Sol. Phys. 187 (July), 229–260, 1999.

Hidalgo, M.A. A study of the expansion and distortion of the cross section of magnetic clouds in the interplanetary medium. J. Geophys. Res. 108 (August), 1320, 2003.

Hidalgo, M.A., Cid, C., Medina, J., Viñas, A.F. A new model for the topology of magnetic clouds in the solar wind. Sol. Phys. 194 (May), 165–174, 2000.

Hidalgo, M.A., Cid, C., Viñas, A.F., Sequeiros, J. A non-force free approach to the topology of magnetic clouds in the solar wind. J. Geophys. Res. 107 (January), 1029, 2002a.

Hidalgo, M.A., Nieves-Chinchilla, T., Cid, C. Elliptical cross-section model for the magnetic topology of magnetic clouds. Geophys. Res. Lett. 29 (July), 15, 2002b.

Hu, Q., Sonnerup, B.U.Ö Reconstruction of magnetic flux ropes in the solar wind. Geophys. Res. Lett. 28 (February), 467–470, 2001.

Hu, Q., Sonnerup, B.U.Ö Reconstruction of magnetic clouds in the solar wind: orientations and configurations. J. Geophys. Res. 107 (July), 1142, 2002.

Hundhausen, A.J. The solar wind. in: Kivelson, M.G., Russell, C.T. (Eds.), Introduction to Space Physics. Cambridge University Press, Cambridge, pp. 91–128, 1995.

Janoo, L., Farrugia, C.J., Torbert, R.B., Quinn, J.M., Szabo, A., Lepping, R.P., Ogilvie, K.W., Lin, R.P., Larson, D., Scudder, J.D., Osherovich, V.A., Steinberg, J.T. Field and flow perturbations in the October 18–19, 1995, magnetic cloud. J. Geophys. Res. 103 (August), 17249–17260, 1998.

Jones, G.H., Rees, A., Balogh, A., Forsyth, R.J. The draping of heliospheric magnetic fields upstream of coronal mass ejecta. Geophys. Res. Lett. 29 (June), 1520, 2002.

Klein, L.W., Burlaga, L.F. Interplanetary magnetic clouds at1 AU. J. Geophys. Res. 87 (February), 613–624, 1982.

Larson, D.E., Lin, R.P., McTiernan, J.M., McFadden, J.P., Ergun, R.E., McCarthy, M., Rème, H., Sanderson, T.R., Kaiser, M., Lepping, R.P., Mazur, J. Tracing the topology of the October

18–20,1995, magnetic cloud with $\sim$0.1–10^2 keV electrons. Geophys. Res. Lett. 24, 1911–1914, 1983.

Lepping, R.P., Berdichevsky, D.B., Szabo, A., Arqueros, C., Lazarus, A.J. Profile of an average magnetic cloud at 1 AU for the quiet solar phase: wind observations. Sol. Phys. 212 (February), 425–444, 2003.

Lepping, R.P., Burlaga, L.F., Jones, J.A. Magnetic field structure of interplanetary magnetic clouds at 1 AU. J. Geophys. Res. 95, 11957–11965, 1990.

Lepping, R.P., Burlaga, L.F., Szabo, A., Ogilvie, K.W., Mish, W.H., Vassiliadis, D., Lazarus, A.J., Steinberg, J.T., Farrugia, C.J., Janoo, L., Mariani, F. The Wind magnetic cloud and events of October 18–20, 1995: interplanetary properties and as triggers for geomagnetic activity. J. Geophys. Res. 102 (July), 14049–14064, 1997.

Lundquist, S. Magnetohydrostatic fields. Ark. Fys. 2, 361–365, 1950.

Luoni, M.L., Mandrini, C.H., Dasso, S., van driel-Gesztelyi, L., Démoulin, P. Tracing magnetic helicity from the solar corona to the interplanetary space. J. Atmos. Sol. Terr. Physics, in press, 2005.

Mandrini, C.H., Demoulin, P., van Driel-Gesztelyi, L., Schmieder, B., Cauzzi, G., Hofmann, A. 3D magnetic reconnection at an X-ray bright point. Sol. Phys. 168 (September), 115–133, 1996.

Mandrini, C.H., Pohjolainen, S., Dasso, S., Green, L.M., Démoulin, P., van driel-Gesztelyi, L., Copperwheat, C., Foley, C. Interplanetary flux rope ejected from an X-ray bright point. Astron. Astrophys. 434, 725–740, 2005.

Marsden, R.G., Sanderson, T.R., Tranquille, C., Wenzel, K.-P, Smith, E.J. ISEE 3 observations of low-energy proton bidirectional events and their relation to isolated interplanetary magnetic structures. J. Geophys. Res. 92, 11009–11019, 1987.

Marubashi, K. Interplanetary magnetic flux ropes and solar filaments. in: Crooker, N., Joselyn, J.A, Feynman, J. (Eds.), Coronal Mass Ejections, Geophysical Monograph, vol. 99. American Geophysical Union, Washington, DC, pp. 147–156, 1997.

Matthaeus, W.H. Magnetic helicity and homogeneous turbulence models. in: Brown, M.R., Canfield, R.C., Pevtsov, A.A. (Eds.), Magnetic Helicity in Space and Laboratory Plasmas, Geophysical Monograph, vol. 111. American Geophysical Union, Washington, DC, pp. 247–255, 2000.

Montgomery, M.D., Asbridge, J.R., Bame, S.J., Feldman, W.C. Solar wind electron temperature depressions following some interplanetary shock waves: evidency for magnetic merging?. J. Geophys. Res. 79 (November), 3103–3110, 1974.

Mulligan, T., Russell, C.T. Multispacecraft modeling of the flux rope structure of interplanetary coronal mass ejections: cylindrically symmetric versus nonsymmetric topologies. J. Geophys. Res. 106 (June), 10581–10596, 2001.

Osherovich, V., Burlaga, L.F. Magnetic clouds. in: Crooker, N., Joselyn, J.A., Feynman, J. (Eds.), Coronal Mass Ejections, Geophysical Monograph, vol. 99. American Geophysical Union, Washington, DC, pp. 157–168, 1997.

Osherovich, V.A., Farrugia, C.J., Burlaga, L.F., Lepping, R.P., Fainberg, J., Stone, R.G. Polytropic relationship in interplanetary magnetic clouds. J. Geophys. Res. 98 (September), 15331–15342, 1993.

Pilipp, W.G., Muehlhaeuser, K.-H., Miggenrieder, H., Montgomery, M.D., Rosenbauer, H. Unusual electron distribution functions in the solar wind derived from the HELIOS plasma experiment – double-strahl distributions and distributions with an extremely anisotropic core. J. Geophys. Res. 92 (February), 1093–1101, 1987.

Press, W.H., Teukolsky, S.A., Vetterling, W.T., Flannery, B.P. Numerical Recipes. Cambridge University Press, New York, 1992.

Richardson, I.G., Cane, H.V. Regions of abnormally low proton temperature in the solar wind (1965–1991) and their association with ejecta. J. Geophys. Res. 100 (December), 23397–23412, 1995.

Richardson, I.G., Farrugia, C.J., Cane, H.V. A statistical study of the behavior of the electron temperature in ejecta. J. Geophys. Res. 102 (March), 4691–4700, 1997.

Riley, P., Linker, J.A., Mikić, Z., Odstrcil, D., Zurbuchen, T.H., Lario, D., Lepping, R.P. Using an MHD simulation to interpret the global context of a coronal mass ejection observed by two spacecraft. J. Geophys. Res. 108 (July), 1272, 2003.

Rust, D.M. Spawning and shedding helical magnetic fields in the solar atmosphere. Geophys. Res. Lett. 21 (February), 241–244, 1994.

Scherrer, P.H., Bogart, R.S., Bush, R.I., Hoeksema, J.T., Kosovichev, A.G., Schou, J., Rosenberg, W., Springer, L., Tarbell, T.D., Title, A., Wolfson, C.J., Zayer, I.MDI Engineering Team The solar oscillations investigation – michelson doppler imager. Sol. Phys. 162, 129–188, 1995.

Smith, C.W. solar-cycle, radial and longitudinal variations of magnetic helicity: IMF observations. in: Brown, M.R., Canfield, R.C., Pevtsov, A.A. (Eds.), Magnetic Helicity in Space and Laboratory Plasmas, Geophysical Monograph, vol. 111. American Geophysical Union, Washington, DC, pp. 239–245, 2000.

Sonnerup, B.U., Cahill, L.J. Magnetosphere structure and attitude from Explorer 12 observations. J. Geophys. Res. 72 (January), 171–183, 1967.

Sturrock, P.A. Plasma Physics: An Introduction to the Theory of Astrophysical, Geophysical and Laboratory Plasmas. Cambridge University Press, New York, 1994.

Taylor, J.B. Relaxation of toroidal plasma and generation of reverse magnetic field. Phys. Rev. Lett. 33 (19), 1139–1141, 1974.

Torsti, J., Riihonen, E., Kocharov, L. The 1998 May 2–3 magnetic cloud: an interplanetary ''highway'' for solar energetic particles observed with SOHO/ERNE. ApJ 600 (January), L83–L86, 2004.

van Driel-Gesztelyi, L., Démoulin, P., Mandrini, C.H. Observations of magnetic helicity. Adv. Space Res. 32, 1855–1866, 2003.

van Driel-Gesztelyi, L., Manoharan, P.K., Démoulin, P., Aulanier, G., Mandrini, C.H., Lopez-Fuentes, M., Schmieder, B., Orlando, S., Thompson, B., Plunkett, S. Initiation of CMEs: the role of magnetic twist. J. Atmos. Terr. Phys. 62 (November), 1437–1448, 2000.

Vandas, M., Fischer, S., Dryer, M., Smith, Z., Detman, T. Simulation of magnetic cloud propagation in the inner heliosphere in two-dimensions 1: a loop perpendicular to the ecliptic plane. J. Geophys. Res. 100 (July), 12285–12292, 1995.

Vandas, M., Geranios, A. November 17–18, 1975, event: a clue to an internal structure of magnetic clouds?. J. Geophys. Res. 106 (February), 1849–1858, 2001.

Vandas, M., Romashets, E.P. A force-free field with constant alpha in an oblate cylinder: a generalization of the Lundquist solution. Astron. Astrophys. 398 (February), 801–807, 2003.

Wei, F., Liu, R., Fan, Q., Feng, X. Identification of the magnetic cloud boundary layers. J. Geophys. Res. 108 (June), 1263, 2003.

Yurchyshyn, V.B., Wang, H., Goode, P.R., Deng, Y. Orientation of the magnetic fields in interplanetary flux ropes and solar filaments. ApJ 563 (December), 381–388, 2001.

Zhao, X.P., Hoeksema, J.T., Marubashi, K. Magnetic cloud B_s events and their dependence on cloud parameters. J. Geophys. Res. 106 (August), 15643–15656, 2001.

Zwickl, R.D., Asbridge, J.R., Bame, S.J., Feldman, W.C., Gosling, J.T., Smith, E.J. Plasma properties of driver gas following interplanetary shocks observed by ISEE-3. in: Neugebauer, M. (Ed.), Solar Wind Five Conference, NASA Conf. Publi., CP-2280. NASA Conference Publications, Washington, DC, pp. 711–717, 1983.